33rd Annual International Conference of the IEEE EMBS
Boston, Massachusetts USA, August 30 - September 3, 2011

Diffusion Kurtosis Imaging Discriminates Patients with White Matter Lesions from Healthy Subjects

Armin Iraji*, Esmaeil Davoodi-Bojd[1], Hamid Soltanian-Zadeh[1,2], Gholam-Ali Hossein-Zadeh[1], Quan Jiang[3]

***Abstract*—This work illustrates that DKI reveals white matter lesions and also discriminates healthy subjects from patientswith white matter lesions. To show this capability, we have investigated DKI images of a healthy subject and apatient with white matter lesions. The analysis was performed both between and within subjects. Regions of Interest (ROIs) for lesion and normal white matterin the patient images are selected manually (for within subject study) and also the corresponding ROIs in the healthy subject are defined (for between subject study). The results of comparing the estimated values for apparent diffusion and kurtosis parameters show that both D_{app} and K_{app} can distinguish normal and abnormal tissues. K_{app} (D_{app}) of the normal regions is greater (lower) than that ofthe abnormal regions. Another investigation over all voxels in the brain shows an important feature of kurtosis in determining white matter lesions.**

I. Introduction

Magnetic Resonance Imaging (MRI) is a state of the art imaging method for detecting white matter lesions and has a higher sensitivity compared to Evoked Potential (EP) evaluation based methods. One of the well-known MRI-based techniques of detecting white matter lesionsis T2 weighted imaging. Despite high performance in providing desired data, this technique is incapable of discriminating between white matter lesions in Multiple Sclerosis (MS) and other pathologies (Orrison, 2000). Diffusion imaging is one of the complicated imaging techniques applied to cope with limitations of usual MRI techniques in evaluating white matter lesions (Zipp, 2009). Several studies declared that using DW-MRI the amount of diffusivity in apparently healthy tissue of white brain tissue (NAMW) is increased, which indicates high sensitivity of this technique compared to other MRI methods (Filippi and Agosta, 2009; Zipp, 2009).

Jensen and Helpern (2003) used "kurtosis imaging" as an important criterion for detection of deviation from the Gaussian shape. Diffusion Kurtosis Imaging (DKI), using second order approximation of displacement distribution of water, calculates apparent diffusion coefficient and apparent diffusion kurtosis. Some major advantages of this method which made it popular among researchers are its reasonable acquisition time and calculation of deviation from Gaussian diffusion (kurtosis).

Manuscript received April15, 2011.

*Control and Intelligent Processing Center of Excellence, School of Electrical and Computer Engineering, University of Tehran, Tehran 14395-515, Iran (+989177118747; e-mail: armin.iraji@ut.ac.ir).

[1]Control and Intelligent Processing Center of Excellence, School of Electrical and Computer Engineering, University of Tehran, Tehran 14395-515,Iran (e-mails:es.davoodi@ut.ac.ir,hszadeh@ut.ac.ir, ghzadeh@ut.ac.ir).

[2]Image Analysis Laboratory, Radiology Department, Henry Ford Hospital, Detroit, MI 48202, USA (e-mail: hamids@rad.hfh.edu).

[3]Neurology Department, Henry Ford Hospital, Detroit, MI 48202, USA (e-mail: qjiang1@hfhs.org).

A benefit of kurtosis measurement is that Gaussian distribution intrinsically shows unlimited and free diffusion, thus this feature can reveal the level of diffusion restriction. Since the profile of restriction depends on the tissue structure, this feature can be considered as a criterion for determining the underlying structure of the tissues, noninvasively. Moreover, many of disorders affect fibers structures which make diffusion non-Gaussian, hence, several studies have shown that kurtosis can distinguish between healthy and patient subjects (Jensen et al, 2005; Lu et al, 2006; Falangola et al, 2007a and 2007b).

In this work, we analyze the values of apparent diffusion and kurtosis parameters in the normal and abnormal white matter tissue.

II. Material and Methods

For conventional pulsed-field gradient spin echo sequence, which is used in diffusion-weighted imaging, the logarithm of signal intensity is equal to (Jensen and Helpern, 2003):

$$\ln[S(b)] = \ln[S(0)] - bD_{app} + (1/6)b^2(D_{app})^2 K_{app} + O(b^3) \qquad (1)$$

where D_{app} is the apparent diffusion coefficient and K_{app} is the apparent kurtosis coefficient. As in the Taylor series,since higher order terms have a lower contribution in the approximation of the original function, terms with higher order than the second order are neglected, conventionally (Jensen and Helpern, 2003). Therefore, we have:

$$\ln\left(\frac{S_b}{S_0}\right) = -bD_{app} + (\frac{1}{6})b^2 {D_{app}}^2 K_{app} \qquad (2)$$

For estimating D_{app} and K_{app} parameters at each applied diffusion gradient direction, at least two different b-value DW images should be acquired. Therefore, the larger number of different b-value images, the more robust estimation of these parameters. We use Least Square (LS) estimation for computing the parameters at each applied diffusion gradient direction.

Diffusion tensor is a symmetric 3x3 tensor thathas 6 independent components. Thus, for computing its unknown components, we need at least 6 DW images in 6 different gradient directions and one baseline image, S_0 (without any gradient). Jensen et al (2005) computed the diffusion tensor from DKI. In this method, suppose the k^{th} gradient direction is $[n_1^{(k)} n_2^{(k)} n_3^{(k)}]'$ and its estimated apparent diffusion parameters are $D_{app}^{(k)}$. Having all of these values, the diffusion tensor components, D_{ij}^{app}, can be estimated using the following set of linear equations (Falangola et al, 2007b):

$$D_{app}^{(k)} = \sum_{i=1}^{3}\sum_{j=1}^{3} n_i^{(k)} n_j^{(k)} D_{ij}^{app} \quad (3)$$

Similar to conventional DTI processing methods, the eigen-values (λ_1, λ_2, λ_3) and eigen-vectors of this tensor are calculated as its basic descriptors. Two main popular scalar parameters of diffusion tensor are defined as Fractional Anisotropy (FA) and Mean Diffusivity (MD) which are calculated using the following equations (Basser et al, 2002):

$$FA = \sqrt{\frac{1}{2}} \frac{\sqrt{(\lambda_1 - \lambda_2)^2 + (\lambda_1 - \lambda_3)^2 + (\lambda_2 - \lambda_3)^2}}{\sqrt{(\lambda_1^2 + \lambda_2^2 + \lambda_3^2)}} \quad (4)$$

$$MD = Trace(D) = \frac{\lambda_1 + \lambda_2 + \lambda_3}{3} \equiv \overline{D}^{app} \quad (5)$$

In our experiment, we acquired *S(b)* in 15 directions each with five different b-values 500, 1000, 1500, 2000, 2500, similar to what is used conventionally in kurtosis imaging. Images were acquired from a healthy subject and a patient with white matter lesions (theimages were taken in 3-months periods) with a voxel resolution of (0.9766x0.9766x2.6) whichgives 256x256x30 volumes. All images were acquired using a 3T GE MRI system atHenry Ford Hospital, Detroit, Michigan, USA.

A. Between Subject Comparison

White matter lesions that usually appear in the regions around the ventricles can be seen in the T2 weighted images (Orrison, 2000). In our experiment, we selected the abnormal regions according to T2 images of the patient manually. The selected ROIs are shown in Figure 1 (a). Moreover, as we want to compare the different parameters within these regions among healthy subject and patient images, we also extracted similar regions in the healthy T2 weighted images manually. There is not an exact correspondence between the selected ROIs in the healthy subject and the patient, however, the size of the regions are large enough to verify that most of the voxels within the two corresponding ROIs belong to identical anatomical structures. Figure 1 (b) shows the selected ROIs for the healthy subject that correspond the ROIs in Figure 1 (a).

B. Within Subject Comparison

Another worthy comparison study between abnormal and healthy tissues is to compare the parameters of an abnormal region with a normal one within the patient image. Therefore, we also select some ROIs in the patient image which appear to be normal and healthy. In Figure 1 (c), these normal appearing ROIs are shown.

Finally, for evaluating the quality and capabilities of kurtosis in detecting disease, the apparent kurtosis and apparent diffusion parameters for the voxels in all ROIs are estimated. For better comparison, the Fractional Anisotropy (FA) and Mean Diffusivity (MD) parameters of the diffusion tensor are also computed using equations (4) and (5).

III. Results and Discussion

As the first step of our investigation, in Figure 2 the mean amplitude of the diffusion signals for different b-values in the selected ROIs are shown for both within subject comparison (Figure 2 (a)) and between subject comparison (Figure 2 (b)). As illustrated in these figures, the amplitudes of the signal in abnormal regions are always less than apparent healthy ones which imply that the disease has serious effects on the tissue structure in the lesions. Moreover, they show the intensity differences between healthy subject and patient. As depicted, the image intensitydecreases as time goes on.

In order to evaluate the quality and capabilities of kurtosis in detecting the disease, the histograms of apparent kurtosis and apparent diffusion values in the lesion regions of the patient and the corresponding regions of the healthy subject are calculated. As illustrated in Figure 3, both D_{app} and K_{app} have distinct histograms for the healthy subject and the patient, justifying the ability of these diffusion parameters in separating healthy regions from abnormal ones. In Table 1, means and standard deviations of D_{app} and K_{app} are presented for all selected regions illustrating differences between the diffusion and kurtosis parameters of the normal and abnormal regions.

So far, we showed that both D_{app} and K_{app} parameters can distinguish between the normal and abnormal regions. To investigate capability of these parameters to separate patients from healthy subjects, we calculate their histograms for all voxels within the brain. In Figure 4, the histograms for D_{app} and K_{app} and also FA are shown. The results reveal that there is adiscriminating peak in the patient data caused by disease through affecting brain tissue and deviating diffusion from Gaussianity. This feature is not seen in the histograms of the mean diffusion and FA. Therefore, kurtosis is superior to the diffusion coefficient in separating patients from healthy subjects.

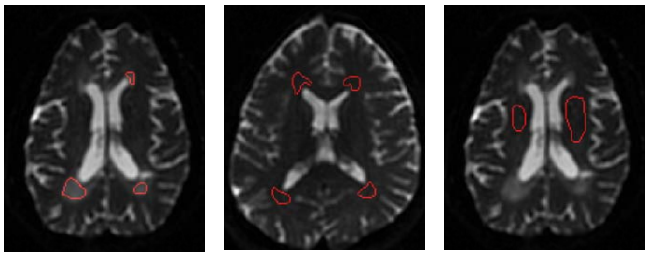

(a) (b) (c)

Figure 1. The selected ROIs for between and within subject comparison overlaid on T2 weighted images. In (a), the ROIs represent abnormal regions in a patient. In (b), the ROIs represent normal regions in a healthy subject. In (c), the ROIs represent normal appearing regions in a patient.

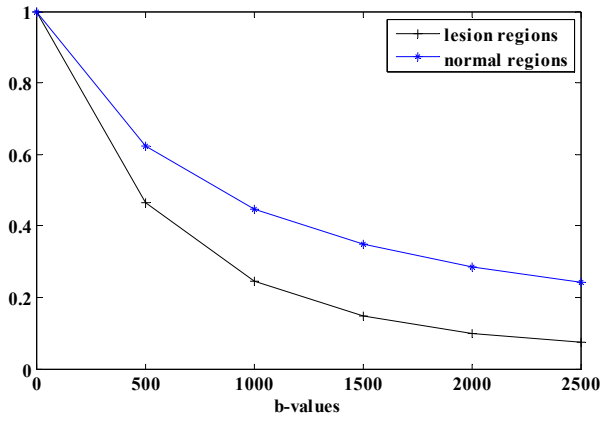

(a)

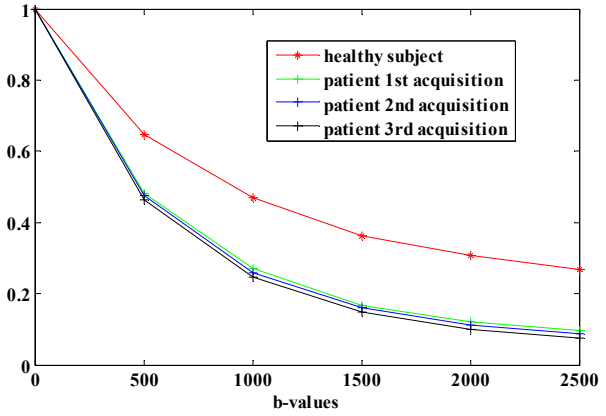

(b)

Figure 2. The mean amplitude of the diffusion signals for different b-values in the selected ROIs for both within subject comparison (a) and between subject comparison (b). In (a), the signal amplitudes for the lesion regions were computed by averaging over all three acquisition times. These figures illustratethe effects of thedisease on the tissue properties.

Table 1. Means and standard deviations of diffusion and kurtosis parameters in the selected ROIs. The last column is the number of voxels within each ROI.

	Acquisition	D (µm2/ms)	K	No. Voxels
Healthy sub.	-	0.9320 ±0.3105	0.952 ±0.802	3925
Lesion ROIs	1st	1.5782 ±0.2698	0.600 ±0.168	4187
	2nd	1.6074 ±0.2819	0.553 ±0.260	
	3rd	1.6570 ±0.2488	0.521 ±0.128	
Normal ROIs	1st	0.9723 ±0.3157	0.865 ±0.772	2151
	2nd	0.9696 ±0.2984	0.748 ±1.066	
	3rd	0.9719 ±0.3100	0.884 ±0.676	

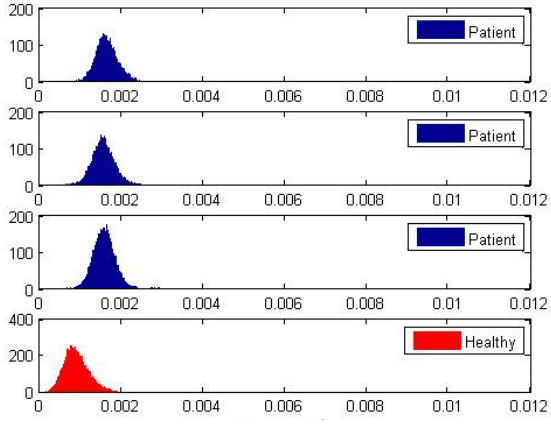

(a) Apparent diffusion histograms

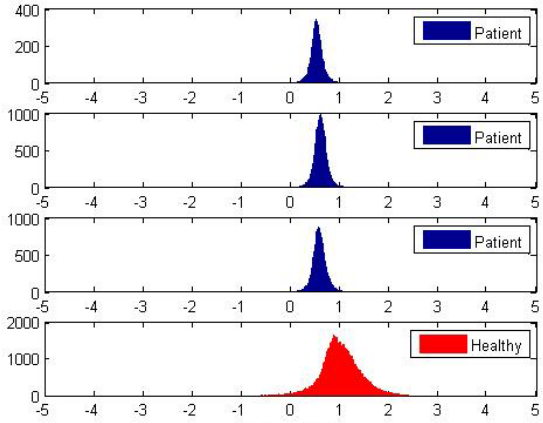

(b) Apparent kurtosis histogram

Figure 3. Histograms of estimated values of D_{app} and K_{app} in the selected regions of the healthy subject and the patient. For the patient, the histograms are shown for each acquisition time. These histograms show the capability of K_{app}, as well as D_{app}, for discriminating lesion regions from the healthy ones.

IV. Conclusion

In this work, we illustrated that kurtosis reveals abnormal white matter regions in the brain. To show this capability, we investigated DKI data of ahealthy subject and a patient with white matter lesions. The analysis was performed both between subjects and within subject. For between subject comparison, some ROIs on the lesions of the patient T2 weighted images were selected manually. Then, the corresponding ROIs in the healthy subject were defined accordingly. For within subject comparison, some ROIs on normal appearing white matter were used. Diffusion and kurtosis parameters were computed in each ROI and their histograms and statistical parameters were compared. The results showed that both D_{app} and K_{app} distinguish normal and abnormal tissues. K_{app} (D_{app}) in the normal regions was greater (lower) than in the abnormal regions. Another investigation over all voxels in the brain showed an

important feature of the kurtosis in determining distinguishing patient from control. Our results indicated that there was a discriminating peak in the histograms of K_{app} calculated from patient's images. This peak was generated by the disease through affecting brain tissue and deviating diffusion from Gaussianity. This feature was not seen in the histograms of mean diffusivity and FA. Therefore, kurtosis may besuperior to other diffusion confidents in separating healthy subjects from patients.

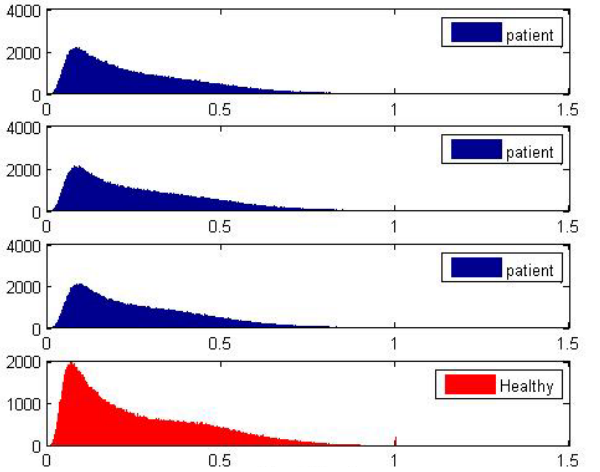

(a) FA histograms

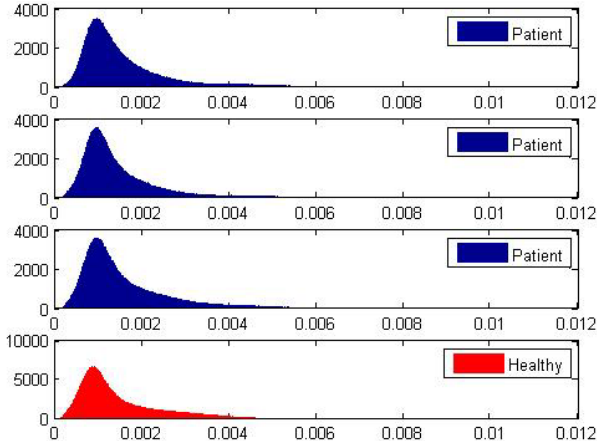

(b) D_{app} histograms

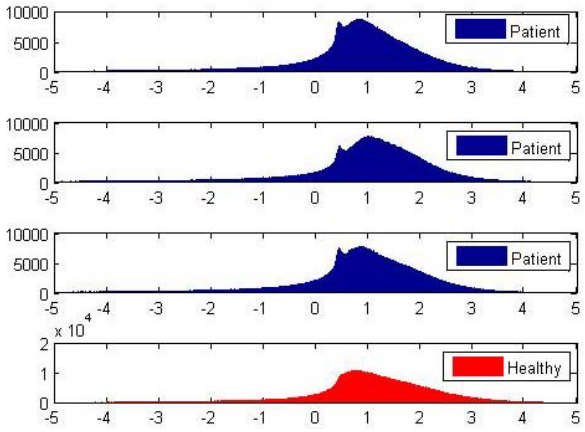

(c) K_{app} histograms

Figure 4. Histograms of estimated values of D_{app} and K_{app} in all voxels of the brain of the healthy subject and the patient in three acquisition times. Note that the histogram of K_{app} may be used to determine a subject has white matter abnormalityor not.

REFERENCES

[1] P.J. Besser and D.K. Jones, "Diffusion-tensor MRI: theory, experimental design and data analysis –a technical review,"*NMR Biomed*, vol. 15, pp. 456-467, 2002.

[2] M.F. Falangola, C. Branch, J.H. Jensen, C. Hu, L. Xuan, K. Duff, R. Nixon, and J.A. Helpern, "Assessment of brain microstructure in a transgenic mouse model of β-Amyloid deposition,"*Proc Intl Soc Mag Reson Med 15,* pp. 310, 2007a.

[3] M.F. Falangola, A. Ramani, A. Dlmartino, J.H. Jensen, J.S. Babb, C. Hu, K.U. Szulc, F.X. Castellanos, and J.A. Helpern, "Age-related patterns of change in brain microstructure by diffusional kurtosis imaging,"*Proc Intl Soc Mag Reson Med 15,* pp.667, 2007b.

[4] M. Filippi and F. Agosta, "Magnetic resonance techniques to quantify tissue damage, tissue repair, and functional cortical reorganization in multiple sclerosis," *Prog Brain Res,* vol. 175, pp. 465-482, 2009.

[5] J.H. Jensen, J.A. Helpern,A. Ramani,H. Lu, and K. Kaczynski, "Diffusional kurtosis imaging: the quantification of non-Gaussian water diffusion by means of magnetic resonance imaging," *MagnReson Med,* vol. 53, pp. 1432-1440, 2005.

[6] J.H. Jensen and J.A. Helpern,"Quantifying non-Gaussian water diffusion by means of pulsed-field-gradient MRI," *Proc Intl Soc Mag Reson Med,* vol. 11, pp. 2154, 2003.

[7] H. Lu, J.H. Jensen, A. Ramani, and J.A. Helpern, "Three-dimensional characterization of non-Gaussian water diffusion in humans using diffusion kurtosis imaging," *NMR Biomed,*vol. 19, pp. 236-247, 2006

[8] W.W. Orrison,"Neuroimaging," vol. 1&2, W. B. Saunders Company, Philadelphia.

[9] F. Zipp, "A new window in multiple sclerosis pathology: non-conventional quantitative magnetic resonance imaging outcomes," *J NeurolSci*, vol. 287, pp. 24-29, 2009.